*Proc. Natl. Acad. Sci. USA*
Vol. 94, pp. 6880–6885, June 1997
Immunology

# The three-dimensional structure of an H-2L$^d$-peptide complex explains the unique interaction of L$^d$ with beta-2 microglobulin and peptide

GANESARATNAM K. BALENDIRAN[†‡], JOYCE C. SOLHEIM[‡§], AIDEEN C. M. YOUNG[‡¶], TED H. HANSEN[§], STANLEY G. NATHENSON[¶], AND JAMES C. SACCHETTINI[†]

[†]Department of Biochemistry and Biophysics, Texas A&M University, College Station, TX 77843; [§]Department of Genetics, Washington University School of Medicine, St. Louis, MO 63110; and [¶]Department of Microbiology and Immunology and Department of Cell Biology, Albert Einstein College of Medicine, Bronx, NY 10461

*Contributed by Stanley G. Nathenson, April 21, 1997*

**ABSTRACT** **Solution at 2.5-Å resolution of the three-dimensional structure of H-2L$^d$ with a single nine-residue peptide provides a structural basis for understanding its unique interaction with beta-2 microglobulin ($\beta_2$m) and peptide. Consistent with the biological data that show an unusually weak association of L$^d$ with $\beta_2$m, a novel orientation of the $\alpha1/\alpha2$ domains of L$^d$ relative to $\beta_2$m results in a dearth of productive contacts compared with other class I proteins. Characteristics of the L$^d$ antigen-binding cleft determine the unique motif of peptides that it binds. L$^d$ has no central anchor residue due to the presence of several bulky side chains in its mid-cleft region. Also, its cleft is significantly more hydrophobic than that of the other class I molecules for which structures are known, resulting in many fewer H-bonds between peptide and cleft residues. The choice of Pro as a consensus anchor at peptide position 2 appears to be related to the hydrophobicity of the B pocket, and to the unique occurrence of Ile (which mirrors Pro in its inability to form H-bonds) at position 63 on the edge of this pocket. Thus, the paucity of stabilizing H-bonds combined with poor complementarity between peptide postion 2 Pro and the B pocket contribute to the weak association between L$^d$ and its peptide antigen. The unique structural interactions of L$^d$ with $\beta_2$m and peptide could make L$^d$ more suited than other classical class I molecules to play a role in alternative pathways of antigen presentation.**

The recognition of foreign antigens by the cellular immune system requires their presentation as short peptides by major histocompatibility complex (MHC) class I molecules to the T cell receptors (TCR) of cytotoxic T lymphocytes. Class I molecules are heterotrimeric structures with (*i*) a highly polymorphic membrane-bound heavy chain that is MHC encoded, (*ii*) a relatively nonpolymorphic, soluble light chain beta-2 microglobulin ($\beta_2$m) that is non-MHC encoded, and (*iii*) a peptide of 8-11 amino acids (cf. ref. 1). Assembly of this trimeric complex occurs in the endoplasmic reticulum (ER), and peptide must remain associated for stable class I complexes to be expressed at the cell surface. The first solution of the three-dimensional (3D) structure of the class I molecule revealed a cleft formed by parallel $\alpha$-helices supported by a floor of $\beta$-strands (2, 3). The length of this cleft is virtually identical in all class I molecules due to the presence of predominantly aromatic residues at both ends (2-8). In all the structures solved thus far, the termini of the peptide are bound in the ends of the groove, where they are involved in an array of H-bonds with conserved cleft residues.

Polymorphic residues of class I molecules are primarily located in the antigen-binding groove (9). Amino acid sequencing of peptides eluted from class I molecules showed that the set of peptides bound by a given allele possesses a characteristic motif with a preference for a particular amino acid at two or more positions (10). These characteristic motif positions, or anchor residues, are buried within complementary pockets in the class I groove and have been designated A through F (11). In every case, one peptide anchor is the carboxyl-terminal peptide position (PC) residue, which is deeply buried in the F pocket. The identity of a second anchor residue and its position in the peptide sequence are a function of the cleft architecture. Thus, the location and characteristics of the pockets in a given class I allele are determined by the particular array of polymorphic residues within the cleft, and they dictate the identity of the anchor residues common to the set of peptides that each allele binds. In this regard, each class I allele has unique interactions with its peptide ligands, resulting in significant allele-specific differences in peptide selection in the ER, as well as peptide-dependent stability at the cell surface.

In this study we have crystallized the mouse H-2L$^d$ molecule, which is known to have several distinguishing properties in regard to its interactions with $\beta_2$m and peptide. The L$^d$ molecule is clearly a classical class I molecule, since it is known to be the restricting element for numerous anti-viral cytolytic responses (12-15) and induces a strong response by allogeneic T cells (16). However, when compared with other class I molecules, L$^d$ has a slower rate of intracellular transport, a weaker association with $\beta_2$m, and a lower level of cell surface expression (17). Because the intracellular mechanisms of class I assembly with $\beta_2$m and peptide are highly interdependent (18), it has been difficult to determine whether the primary defect in L$^d$ expression is poor association with $\beta_2$m, peptide, or both. Peptide elution studies have shown that L$^d$ molecules prefer to bind nonameric peptides with Pro at peptide position 2 (P2) (19), similar to several human HLA-B alleles (20). Interestingly, however, L$^d$ molecules also bind and present to cytotoxic T lymphocytes octameric peptides that lack the P2 Pro anchor (21, 22). To probe the structural basis for the unique biological properties of L$^d$, we have determined the 3D structure of the trimeric complex of L$^d$ with $\beta_2$m and a single abundant endogenous peptide.

## MATERIALS AND METHODS

**Preparation of L$^d$ and $\beta_2$m Protein.** The L$^d$ cDNA sequence coding for amino acids 1-280 was amplified by PCR with the oligonucleotide 5′-GGGAATTCATATGGGCCCACACTC-GATGCGG-3′ and 5-′AGAGGATCCTCATCAAGTGGAC-GGAGGAGGCTC3-′ and sequenced to confirm fidelity. The

The publication costs of this article were defrayed in part by page charge payment. This article must therefore be hereby marked "*advertisement*" in accordance with 18 U.S.C. §1734 solely to indicate this fact.



Abbreviations: $\beta_2$m, beta-2 microglobulin; MHC, major histocompatibility complex; P2, peptide position 2; PC, carboxyl-terminal peptide position; p29, peptide YPNVNIHNF; Flu Np, influenza virus peptide ASNENMETM; rms, root-mean-square; TCR, T cell receptor; ER, endoplasmic reticulum; vdw, van der Waals; 3D, three-dimensional.
‡G.K.B., J.C.S., and A.C.M.Y. contributed equally to this study.

PCR product was cloned into the pET-3a vector at the *Nde*I and *Bam*HI sites and transformed into BL21(DE3)pLysS (Novagen). Amplification of the $\beta_2$m DNA sequence that encodes amino acids 1-99, cloning of the $\beta_2$m DNA into pET-3a, and the transformation of the expression plasmid into BL21(DE3)pLysS has been described (5).

Transformed BL21(DE3)pLysS cells were grown at 37°C in Luria–Bertani medium containing 50 $\mu$g/ml of carbenicillin and 10 $\mu$g/ml of chloramphenicol. Isopropyl $\beta$-D-thiogalactopyranoside (Sigma) was added to a final concentration of 0.5 mM when the culture reached an $OD_{600}$ of 0.6-0.9. Incubation was continued for a further 2-3 hr at which point the cells were harvested, suspended in a cold solution of 20 mM Tris·HCl (pH 8.0), 23% (vol/vol) sucrose, 5 mM EDTA, and 100 $\mu$g/ml lysozyme, and then lysed with a French press. After centrifugation at 15,000 × *g*, the pellet (mainly inclusion bodies) was washed twice with a solution of 20 mM Tris·HCl, 23% (vol/vol) sucrose, 5 mM EDTA, and 0.5% Triton X-100.

**Preparation of the H-2L$^d$ Complex.** To prepare complexes of L$^d$ with $\beta_2$m and the p29 peptide (YPNVNIHNF), aliquots of inclusion bodies containing L$^d$ and $\beta_2$m were dissolved separately in a solution of 20 mM Tris·HCl (pH 8.0) and 8 M urea. The solutions were centrifuged to remove particulate material. Synthetic, HPLC-purified p29 peptide was dissolved in 20 mM Tris·HCl (pH 8.0). L$^d$, $\beta_2$m, and peptide were then mixed in a 1:1:3 molar ratio and the solution was diluted to a final concentration of 20 mM Tris·HCl (pH 8.0), 4 M urea, and 250 $\mu$g/ml of total protein. The mixture was dialyzed using Spectra/Por CE dialysis tubing with a molecular weight cutoff of 500 against a 10-fold larger volume of 10 mM potassium phosphate (pH 7.4). The complex was then purified by Superdex G-75 (Pharmacia) size exclusion chromatography followed by Mono Q (Pharmacia) cation exchange chromatography.

**Crystallization of the L$^d$ Complex.** The conditions for the crystallization of the MHC–peptide complex were discovered using the sparse scan technique (23) with the hanging drop vapor diffusion method. Single crystals were obtained by mixing the purified complex at 10 mg/ml in a 1:1 ratio with a precipitant solution containing ≈1.4 M $Na_2SO_4$, and 2-8% glycerol at pH 8.5 and suspended over 1 ml of the same precipitant solution.

**Data Collection and Processing.** The L$^d$–$\beta_2$m–p29 complex crystals have been characterized as orthorhombic, space group $P2_12_12$ with unit cell dimensions a = 150.1 Å, b = 87.2 Å, c = 80.3 Å, $\alpha = \beta = \gamma = 90°$ and two molecules of the L$^d$–$\beta_2$m–p29 complex per asymmetric unit. X-ray diffraction data were collected on a Siemens multiwire area detector system coupled to a Rigaku RU-200 rotating anode x-ray generator operating at 55 kV and 85 mA. Diffraction data to 2.4-Å resolution were collected from one crystal of the L$^d$–$\beta_2$m–p29 complex and reduced using the Siemens package XENGEN (Siemens Analytical X-Ray Instruments, Madison, WI). The data set contained 28,578 unique reflections ($I > 2\sigma$) and was 58% complete in the 2.5-2.4-Å resolution shell and contained 26,846 unique reflections ($I > 2\sigma$) to 2.5-Å resolution (75% complete). The entire data set with a redundancy of 2.4 up to 2.4-A resolution has the overall merging R-factor of 9.7% on intensity.

**Structure Solution and Refinement.** The structure of L$^d$–$\beta_2$m–p29 complex was determined by the method of molecular replacement using the program AMORE (24) with the class I molecule H-2D$^b$ containing the heavy chain, light chain, but no peptide as the search model. The rotation function gave two solutions with the top peak having a correlation coefficient of 22.7 at $\alpha = 2.7°$, $\beta = 84.8°$, and $\gamma = 95.8°$, and the second highest peak having a correlation coefficient of 16.2 at $\alpha = 177.5°$, $\beta = 90.0°$, and $\gamma = 276.5°$, corresponding to the two molecules of the asymmetric unit. A subsequent translation search yielded a single solution at Ta = 0.104, Tb = 0.194, and Tc = 0.177 for the first molecule and another single solution at Ta = 0.897, Tb = 0.685, and Tc = 0.679 for the second molecule. Rigid-body minimization using AMoRe including two molecules gave an R-factor of 41.6% and correlation coefficient of 49.0%. The homology module of INSIGHT was used to build the correct sequence of H-2L$^d$. The model was refined using a combination of simulated annealing using X-PLOR (25), and conventional least-squares methods using TNT (26). Model building was performed after 10 cycles of refinement using electron density maps with both 2Fo-Fc and Fo-Fc coefficients. At an R-factor of 21.5%, distinct continuous difference density was observed between the helices of the antigen-presenting domain of the heavy chain in both asymmetric units. As a first step, four Ala residues were built into this density and refinement continued. In subsequent steps, more Ala residues were inserted. Eventually, clear density for one of the motif residues of the peptide—Phe at position 9—was identified and built into the sequence. In subsequent cycles of refinement, difference electron density for the remaining peptide residues could be clearly assigned and the side chains of the rest of the peptide built. The final R-factor was 18.6% with the $R_{free}$ of 27.9%. The final structure has root-mean-square (rms) deviations in bond lengths of 0.014 Å and rms deviations in bond angles of 2.10° and contains a total of 45 water molecules. The main chain atoms of the antigen-presentation domains of both molecules in the asymmetric unit superimpose with an rms deviation of 0.84 Å compared with an rms of 1.1 Å for all of the heavy chain atoms. Since the two molecules do not differ significantly, only one molecule will be considered for future discussion.

## RESULTS AND DISCUSSION

**Overall Structure of H-2L$^d$ Reveals Unique Interdomain Contacts with $\beta_2$m.** To solve the 3D structure of mouse H-2L$^d$ and probe its relationship with $\beta_2$m and peptide, trimeric complexes of L$^d$–$\beta_2$m–p29 were isolated from a bacterial expression system. The abundant endogenous peptide p29 was selected for this analysis because p29 is known to form more stable complexes with L$^d$ than other ligands tested (27). Furthermore, the sequence of p29 conforms to the consensus L$^d$ peptide motif (19). Molecular replacement with the D$^b$ structure (5) was used to solve the 3D structure of the L$^d$–$\beta_2$m–p29 complex. Superposition of 260 C$\alpha$ atoms of the heavy chains of D$^b$ and L$^d$ gave an rms difference of 1.8 Å. The overall structure of L$^d$, as expected, is very similar to that of K$^b$ and D$^b$. However, the interdomain interactions between L$^d$ and $\beta_2$m are very different from those previously described for the K$^b$ or D$^b$ structures (3-5). As shown in Table 1, there are significantly fewer van der Waals (vdw) interactions and H-bonds between the light and heavy chains of L$^d$ than K$^b$ or D$^b$. Furthermore, L$^d$ appears atypical in its paucity of stabilizing interactions between the $\alpha1/\alpha2$ domains and $\beta_2$m (Table 1 and Fig. 1). It is important to note that of the 23 residues of D$^b$ that are involved in hydrophobic and hydrophilic interactions with $\beta_2$m, only Arg-121 is changed to Cys in L$^d$. Thus, the weak association seen between L$^d$ and $\beta_2$m comes mainly from their

Table 1. Intermolecular interactions between heavy chain and $\beta_2$m of H-2K$^b$, H-2D$^b$, and H-2L$^d$

| | H-2K$^b$ | H-2D$^b$ | H-2L$^d$ |
|---|---|---|---|
| Heavy chain: $\beta_2$m | | | |
| vdw | 17 | 24 | 7 |
| H-bonds | 7 | 13 | 10 |
| (no. of MHC residues involved) | (18) | (23) | (13) |
| $\alpha1$:$\beta_2$m | | | |
| vdw | 4 | 8 | 2 |
| H-bonds | 1 | 3 | 1 |
| $\alpha2$:$\beta_2$m | | | |
| vdw | 9 | 8 | 2 |
| H-bonds | 3 | 2 | 1 |
| $\alpha3$:$\beta_2$m | | | |
| vdw | 4 | 8 | 3 |
| H-bonds | 3 | 8 | 8 |

Distances of <4.0 Å for vdw contacts and <3.2 Å for H-bonds.

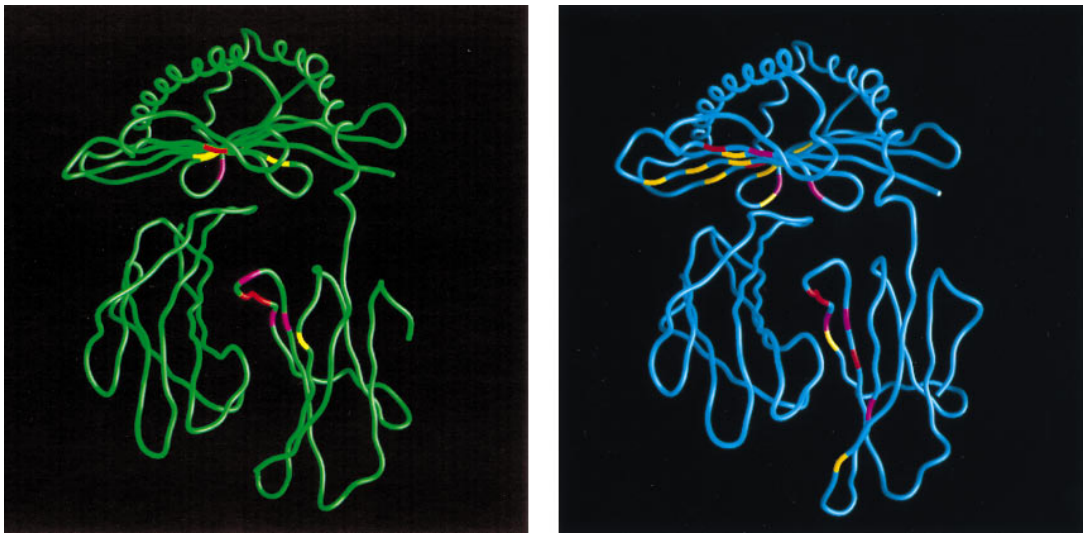

FIG. 1. Comparison of the interactions of $L^d$ versus $D^b$ heavy chains with $\beta_2$m. The C$\alpha$ trace of $L^d/\beta_2$m (*Left*, green) and $D^b/\beta_2$m (*Right*, blue) are shown. The heavy chain residues that interact with $\beta_2$m are highlighted: yellow, vdw; red, H-bonds; pink, both. Domains $\alpha$1 and $\alpha$2 of $L^d$ are related by a 175° rotation followed by a 0.39-Å translation compared with a 177° rotation followed by a 0.12-Å translation for $D^b$ and a 176° rotation followed by a 0.09-Å translation in $K^b$. Furthermore, the $\alpha$3 domain of $L^d$ and $\beta_2$m are related by a 142° rotation and a 13-Å translation, whereas in $D^b$ these domains are related by a 141° rotation and 14-Å translation and in $K^b$ a rotation of 139° and a translation of 14 Å. The decreased number of bonds of $L^d$ versus $D^b$ with $\beta_2$m result from differences in the orientation of the domains.

relative orientation (Fig. 1 legend) and not from polymorphic residues at direct sites of interaction. These results regarding the interactions of $\beta_2$m with $L^d$ provide the structural basis for previous biological observations. For example, $L^d$ more than $D^b$ or other class I molecules, has a propensity to exchange mouse $\beta_2$m for heterologous $\beta_2$m at the cell surface (28). Furthermore, studies of chimeric molecules have indicated that the weak association between $L^d$ and mouse $\beta_2$m maps to the $\alpha1/\alpha2$ domain (17). Thus, the structural and biological data are mutually supportive and clearly demonstrate that the $\alpha1/\alpha2$ domains of $L^d$, compared with $K^b$ or $D^b$, have significantly fewer productive interactions with $\beta_2$m.

**Conformation of the Bound Peptide.** The p29 peptide is bound in the cleft of $L^d$ in an extended conformation with its N terminus bound in the A pocket and the side chain of its PC residue bound deeply within the F pocket. The $\Phi$ and $\psi$ angles of each of the peptide residues indicate that with the exception of P6-Ile (48.6-139.4), all lie in allowed regions of the Ramachandran plot. The backbone trace of this peptide is very similar to that of the influenza virus peptide ASNENMETM (Flu Np) when bound to $D^b$ (5), a molecule highly homologous to $L^d$. When the C$\alpha$ atoms of the antigen presentation domain are superimposed, there is a rms deviation between peptides of 0.8 Å. P3-Asn of the p29 peptide overlaps well with P3-Asn in $D^b$, both pointing into the D pocket beneath $\alpha$2. Peptides eluted from $L^d$ show a preponderance of Asn at the P3 position (19), indicating its importance as a so-called secondary anchor position. The D pocket is fairly exposed near the surface of the cleft, explaining why it imposes less stringency on the peptide residues that are accommodated there than do the primary anchor-containing pockets. P4-Val is directed into external solvent, as is P4-Glu of the $D^b$ peptide, though as a result of differences in the conformation of P5 their backbones are not quite overlapping. P4-Val provides 50.1 $Å^2$ of solvent-accessible surface area, which is 15% of the total accessible surface area of the peptide. The largest difference in the conformations of p29 bound to $L^d$ and the Flu Np peptide bound to $D^b$ is in the orientation of P5, also Asn in both peptides. In p29, P5-Asn is pointing toward the $\alpha$1 helix, whereas in $D^b$, it is an anchor residue pointing down into the cleft, where it forms solvent-mediated H-bonds with Glu-9 and Gln-70. P6-Ile of the p29 peptide is also pointing out of the cleft and is the most solvent accessible of all the residues of the peptide, providing a full 31.4% of the peptide's total solvent accessible surface area. P7H and P8N point toward the $\alpha$2 and $\alpha$1 helices respectively, in which orientation they are also highly coincident with the P7 and P8 residues of the Flu Np peptide bound to $D^b$. We have previously correlated the solvent accessibility of a given peptide residue with its availability for contact by the TCR (3). It is therefore notable that studies using substituted analogues of antigenic peptide nonamers that bind to $L^d$ have defined P5 and P6 residues as primary TCR contacts (cf. ref. 29). These observations are consistent with the solvent accessibility of positions P5 and P6 of the p29 peptide reported here and, furthermore, support a recent model implicating the middle of the peptide as the principal TCR contact region (30, 31).

**The $L^d$ Peptide-Binding Cleft Is Highly Hydrophobic.** The antigen presentation domain of $L^d$ differs from that of $D^b$ at nine residues (positions 63, 66, 77, 80, 97, 99, 114, 150, and 155), of which four are located on the $\alpha$1 helix, two on the $\alpha$2 helix near the C-terminal end of the bound peptide, and three on the floor of the cleft. Six of these residues are polar or charged in $D^b$, but hydrophobic in $L^d$. As a result of its amino acid composition, the $L^d$ cleft is significantly more hydrophobic than that of $D^b$ (Fig. 2), or indeed, any of the MHC class I molecules whose structures have been solved. The grooves of both $D^b$ and $L^d$ are composed of the side chains of the same 35 residues, giving a surface area for the $L^d$ cleft of 1,296 $Å^2$ and the $D^b$ cleft of 1,196 $Å^2$. However, 66% of the surface area of the $L^d$ cleft comes from hydrophobic side chains, while the corresponding value for $D^b$ is 54%. Furthermore, $L^d$ possesses the same hydrophobic ridge composed of residues Tyr-73, Tyr-156, and Trp-147, which is such a prominent feature of the $D^b$ cleft. The architecture of the ridge is almost identical in both alleles, and causes the bound peptide to bulge out of the groove at P6.

It is significant that the p29 peptide forms a total of 14 H-bonds with 10 different $L^d$ cleft residues, whereas the Flu Np peptide forms a total of 22 H-bonds with 18 different $D^b$ cleft residues (Table 2). Clearly, this is a result of the increased hydrophobicity of the $L^d$ cleft, and the dearth of H-bonding capability within it. The N terminus of the peptide is held in pocket A of the cleft via H-bonds between its main chain N and O atoms and the hydroxyl groups of these conserved Tyr residues at positions 7, 159, and 171. The main chain N and O atoms of P9, which are exposed on the surface of the complex as a result of the side chain of the PC residue being buried within the F pocket, are involved in H-bonding interactions with Asn-77, Tyr-84, Thr-143, and Lys-146

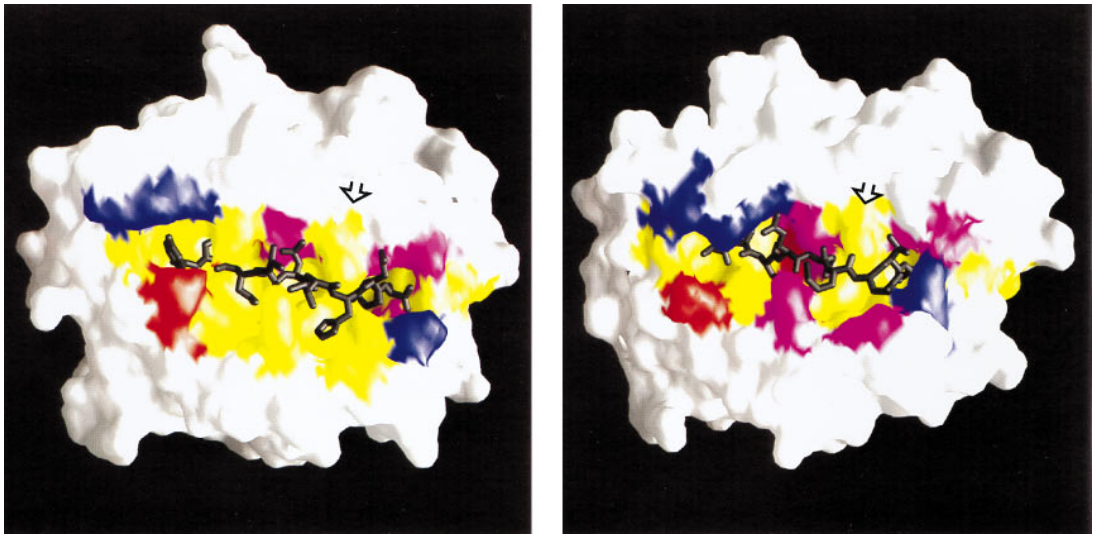

FIG. 2. Comparison of the surface of the ligand-binding sites of $L^d$–p29 (*Left*) and $D^b$–Flu Np (*Right*) complexes. Respective peptides are shown in black. Heavy chain residues that interact with peptide are highlighted: yellow, hydrophobic/aromatic; purple, polar; red, negatively charged; blue, positively charged. The figure was prepared using GRASP (32). The architecture of the ridge (indicated with arrow) is very similar in both $L^d$ and $D^b$.

as well as hydrophobic interactions with Phe-116 and Tyr-123. These H-bonding interactions with conserved residues at both ends of the antigen-binding cleft are largely conserved among all class I structures. In $D^b$, the ND2 atom of Asn-80 H-bonds to the carboxyl group of the PC amino acid. In $L^d$, however, where residue 80 is Thr, this H-bonding capability is lost. Instead, $L^d$ compensates with a different H-bond between the main chain N atom of P9 and ND2 of Asn-77, a H-bond that cannot be formed in $D^b$ where residue 77 is Ser. Overall, however, the unique hydrophobicity of the $L^d$ ligand-binding cleft causes this class I molecule to have fewer opportunities to form productive interactions with peptide.

**Why Is Pro at P2 an Anchor Residue?** The B pocket is made up of the side chains of residues 7, 9, 24, 45, 63, 66, 67, 70, and 99 (11) and properties of residues at these positions determine the architecture of the B pocket in a particular MHC product. The amino acid composition of the B pocket of $L^d$ differs from that of $D^b$ at residues 63 (Ile in $L^d$, Lys in $D^b$), 66 (Ile in $L^d$, Lys in $D^b$), and 99 (Tyr in $L^d$, Ser in $D^b$), but the 3D structures reveal that the topology and size of this pocket is similar in both alleles. In the complex of the p29 peptide bound to $L^d$, Pro at P2 of the peptide is bound in the B pocket and, indeed, it superimposes well with Ser at P2 of the Flu Np peptide in the $D^b$ cleft. Only minor differences in the topography of this pocket are caused by the presence of Ile at position 66 of $L^d$, which protrudes out over the cleft more than Lys at this position in $D^b$. Furthermore, the bulky residue Tyr at position 99 on the floor of the $L^d$ cleft impinges on the edge of the B pocket. In the $D^b$ structure, P2 Ser is involved in several H-bonding interactions with residues of the B pocket (5). Its O and N atoms are involved in H-bonds with side chain

Table 2. H-bonds (distance of 3.2 Å or less is considered) found between the main chain and side chain atoms of the nonapeptides p29, Flu Np, and SEV with the residues of the cleft in the $L^d$, $D^b$ (5), and $K^b$ (4), respectively

| p29 | H-2L$^d$(11,3) | Flu Np | H-2D$^d$(13,9) | SEV | H-2K$^b$(18,3) |
|---|---|---|---|---|---|
| P1Y N | OH–Y171 | P1A N | OH–Y171 | P1F N | OH–Y171 |
| O | OH–Y159 | O | OH–Y159 | | OH–Y7 |
| P2P N | | P2S N | OE2–E63 | O | OH–Y159 |
| O | | O | NZ–K66 | P2A N | OE1–E63 |
| P3N N | OH–Y99 | OG | OE2–E63 | O | NZ–K66 |
| O | OE1–Q70 | | OH–Y45 | P3P N | |
| P4V N | | | OH–Y22 | O | ND2–N70 |
| O | OH–Y155 | P3N N | OG–S99 | | OE2–E24 |
| P5N N | | OD1 | OE1–E9 | P5N N | OD1–N70 |
| O | | | NE2–Q70 | P6Y N | OD1–N70 |
| ND2 | NE2–Q70 | P4E O | NE2–H155 | O | OG–S73 |
| OD1 | OE1–Q70 | P5N N | OE1–Q70 | OH | O–Y7 |
| OD1 | NE2–Q70 | ND2 | OH–Y156 | | OE2–E24 |
| P6I N | | OD1 | NE2–Q97 | | OG–S99 |
| O | | P6M O | NE1–W73 | P8A O | NE1–W147 |
| P7H N | | SD | ND1–H155 | P9L N | OD2–D77 |
| O | NE1–W147 | P7E O | NE1–W73 | | OG1–T80 |
| P8N N | | OE1 | OG–S150 | O | OH–Y84 |
| O | NE1–W147 | P8T O | NE1–W147 | | OG1–T143 |
| P9F N | ND2–N77 | P9M O | ND2–N80 | OT | NZ–K146 |
| O | NZK146 | OT | OH–Y84 | | OG1–T80 |
| O | OG1–T143 | | OG1–T143 | | OD2–D77 |
| O | OH–Y84 | | | | |

Total number of H-bonds involving main chain, side chain atoms are shown in parentheses.

atoms on Glu-63 and Lys-66, both of which interactions are precluded in $L^d$, where both residues are Ile. Furthermore, the side chain O atom of Ser at P2 is involved in one direct H-bond with a side chain O atom of Glu-63, as well as two solvent-mediated H-bonds with Tyr-45 and Tyr-22. Since Pro at P2 of the p29 peptide has an apolar side chain, and its main chain N atom lacks the H-bonding capabilities of a free main chain N atom, all these H-bonds are impossible in the $L^d$ protein.

In the structure of $D^b$, it was observed that the binding of Ser in the B pocket allowed sufficient space for an ordered water molecule with which the side chain of Ser could H-bond. It has been suggested (33) that in $D^b$ this pocket could just as well bind Ser or an amino acid with a longer side chain and that this is why peptides binding to $D^b$ do not show a stringent requirement for Ser at P2. Similarly, even when Pro at P2 of the p29 peptide is bound in pocket B of $L^d$, a small cavity (volume 18.2 $Å^3$, as determined by a 1.4-Å probe) remains between the side chains of residues Ala-67, Tyr-22, Ile-66, and Tyr-45 deep under the $\alpha$1 helix. This is in contrast with the structures of two human alleles, HLA-B*3501 and HLA-B*5301 (7, 8), which also bind peptides with a consensus Pro at P2. In these structures, the shape complementarity between the cleft and the bound Pro residue in the B pocket is very high, with no room for any additional atoms. The B pocket is more shallow in these alleles than in $L^d$, primarily because position 67 is Phe in the human alleles, but Ala in $L^d$. The 3D structures of MHC class I molecules reveal that, in addition to a network of H-bonding interactions, peptide binding requires high complementarity between the anchor residues and their corresponding pockets within the cleft, thus providing binding energy in the form of nonspecific vdw interactions. In the case of $K^b$, for example, a large contribution to the binding of the vesicular stomatitis virus peptide comes from vdw interactions that arise from the highly complementary interactions between P8-Leu and the F pocket and between P5-Tyr and the C pocket. Indeed, all the class I–peptide complexes whose structures have been solved have two principal anchor residues that are highly complementary with the particular pockets in which they reside.

The fact that in the $L^d$/p29 structure a principal peptide anchor position is one with poor complementarity with the cleft raises questions about why Pro is a consensus residue for $L^d$. In this regard, it is notable that $L^d$ is the only allele with a nonpolar residue at position 63. Because in all other MHC class I complexes whose structures have been solved the side chain of this residue is involved in H-bonds with either the side chain or main chain atoms at P2, it is tempting to speculate that one of the factors contributing to the specificity of $L^d$ for Pro with its diminished H-bonding capabilities at P2 is the absence of a H-bonding residue at position 63. It may be that the presence of a residue at position 63 with H-bonding capabilities dictates the identity of the P2 residue with which it will H-bond. Smith *et al.* (8) postulate that Pro at P2 is an anchor residue for HLA-B53 because residue 63 in this allele is Asn, with a shorter side chain than Glu, which is found in the other human alleles. With Asn at position 63, they surmise, the usual H-bonding interactions are abrogated, leading to the choice of Pro as an anchor, for which H-bonding interactions are not a consideration. By similar reasoning, one may justify the choice of Pro at P2 for peptides binding to H-2$L^d$. However, unlike in other MHC class I structures where the peptide is bound via two highly complementary anchors, in $L^d$, although the F pocket is highly complementary for the PC residue of p29, the second principal anchor on which peptide-binding depends, Pro at P2, has imperfect complementarity with the B pocket. It is likely that this results in an overall reduced energy of peptide binding when compared with alleles that bind peptides with two highly complementary anchors.

**Why Do Peptides Binding to $L^d$ *Not* Have a Central Anchor Residue?** The topology of the mid-cleft region where pocket C is located in the MHC class I molecule is primarily dictated by the identity of cleft residues 9, 97, and 99. $K^b$ has Val-9, Val-97, and Ser-99 and hence a spacious C pocket large enough to accommodate the side chain of Tyr as an anchor residue (3, 4). By contrast, $D^b$ has Glu-9, Gln-97, and Ser-99 forming a smaller and more polar C pocket, in which it binds the side chain of an Asn (5). Indeed, $K^b$ and $D^b$ differ from the rest of the human and murine alleles for which consensus peptide ligand sequences are known in that their second peptide anchor position occurs in the middle of the peptide sequence, at P5. The $L^d$ cleft does not have a C pocket in its central cleft region because of the presence of Tyr-99 and Trp-97, which both stick up from the floor of the cleft. These large, bulky residues give rise to a very hydrophobic and shallow mid-cleft region. As a result, P5-Asn of the p29 peptide is not buried within the cleft, consistent with the fact the Asn at P5 is not a consensus residue for peptides binding to $L^d$. Nevertheless, when the p29 peptide is bound, a small cavity remains in the cleft underneath the side chain of P5-Asn of p29, and bounded by Trp-97, Phe-116, Trp-73, and Thr-156, an additional factor in the lack of complementarity between peptide and cleft.

In the $D^b$/Flu Np structure the side chain of the P5-Asn anchor residue H-bonds with the side chains of Tyr-156 and Gln-97, which serve to position it within the cleft (5). In $L^d$, however, residue 97 is Trp and this same bond cannot be formed. Hence, Asn at P5 of the p29 peptide is not an anchor residue for $L^d$ because (*i*) the occurrence of bulky residues in the central cleft region preclude the same positioning of P5-Asn as seen in $D^b$ and (*ii*) the H-bonding interactions that stabilize P5-Asn of the $D^b$ structure within the cleft cannot be formed in $L^d$.

**How Can $L^d$ Bind an Octapeptide?** In our recent study of the Db/Flu Np structure we discussed how a conserved network of H-bonding interactions between its termini and residues of the cleft impose a minimum length requirement on the bound peptide (5). The bulge produced in the backbone of its bound peptide by the hydrophobic ridge in the $D^b$ cleft led us to speculate that alleles possessing such a ridge would be unable to bind peptides of less than nine amino acids in length (5). It is therefore intriguing that although the 3D structure of $L^d$ reveals a hydrophobic ridge, virtually identical to that seen in $D^b$, $L^d$ binds octapeptides. Indeed, two of the well-characterized, naturally processed $L^d$ ligands are octapeptides. The p2Ca peptide (LSPFPFDL) (21) is immunodominant among T cells alloreactive to $L^d$ (34) and the $tum^-$ peptide (QNHRALDL) (22) is a tumor-associated antigen (35). It is curious that in these octapeptides the side chains at P2 are smaller and more flexible than the consensus Pro that occurs at P2 in most nonameric $L^d$ ligands. Furthermore, while the penultimate residue in the nonapeptides that bind to $L^d$ (P8-Asn in p29) is not an anchor residue, both octapeptides have a conserved Asp at their penultimate P7, that is known to function as an anchor residue (29).

It seems likely that for $L^d$ to bind an octameric peptide such that its termini are involved in the same set of stabilizing H-bonds seen in other class I/peptide complexes, some alteration in the structure of its hydrophobic ridge must occur. Repositioning of the residues comprising the ridge may allow the ridge to be flattened or eliminated entirely, so that $L^d$ can bind eight-residue peptides with no imposed backbone bulge. Furthermore, alterations in the hydrophobic ridge in the $L^d$ cleft, induced upon binding an octameric peptide, may be propagated throughout the cleft. As a result, one or more of the side chains of residues comprising the B pocket may be shifted into position to form H-bonds with the side chains of P2-Ser of the p2Ca peptide or with P2-Asn of the $tum^-$ peptide, thereby removing the requirement for a Pro at P2.

**Do $L^d$ Molecules Have a Specialized Role in Antigen Presentation?** We demonstrate here that the association between $L^d$ and the nonapeptide p29 is weaker than that seen for other class I–peptide complexes crystallized thus far. Our data indicate that the weak association between $L^d$ and peptide is due to the hydrophobicity of its cleft residues, which preclude a number of specific H-bonds seen in other complexes. In addition, the shallowness of its cleft precludes a central peptide anchor, and key

H-bonding interactions that stabilize a central anchor are impossible. Thus, the peptide residue that binds in the B pocket must serve as the second principal anchor for nonameric $L^d$ ligands. The hydrophobicity of this pocket is conducive for binding an uncharged residue, and the choice of Pro appears to be related to the inability of Pro to form H-bonds. In every MHC class I complex structure that has been solved, residue 63 (usually Glu) is involved in H-bonding interactions with the P2 peptide residue. In H-$2L^d$, residue 63 is Ile and is therefore matched to the Pro in its inability to form H-bonds. Furthermore, the Pro binds in the B pocket with poor complementarity, as evidenced by the fact that a small cavity remains between the Pro residue and residues at the back of the B pocket when the peptide is bound. Thus, fewer H-bonds and poorer complementarity between peptide and cleft indicate that the p29 peptide is less tightly bound in the cleft of $L^d$ than other peptides bound to their respective class I alleles. Since p29 is known to stabilize $L^d$ better than other known $L^d$ ligands (27), we surmise that other $L^d$ ligands may form even fewer H-bonds and are less complementary with the $L^d$ cleft.

The weak interaction of $L^d$ with peptides is likely to be the primary factor determining its lower level of expression on the cell surface. Surface expression of $L^d$ is 2- to 5-fold lower than that of other classical class I molecules (17). Furthermore, stable surface expression of class I is clearly dependent upon peptide occupancy (36). The weak association of $L^d$ with peptide described here would be predicted to result in peptide dissociation and turnover of $L^d$ at the cell surface. In support of this prediction, the surface half-life of $L^d$ is significantly shorter than that of other classical class I molecules (37). Compounding its weak peptide binding, $L^d$ could have problems docking with transporter associated with antigen processing prior to peptide loading, since transporter associated with antigen processing association of class I is $\beta_2$m dependent (38, 39). Thus, the weak association of $L^d$ with $\beta_2$m could indirectly alter peptide binding.

It is intriguing to speculate why $L^d$ is predominantly used by immune T cells in responses to mouse cytomegalovirus, lymphocytic choriomeningitis virus, hepatitis B virus, and vesicular stomatitis virus (12-15). After all, the weak association of $L^d$ for peptide and $\beta_2$m could be considered impediments for optimal antigen presentation to T cells. However, these unique features of $L^d$ might facilitate a more specialized function in alternative pathways of class I antigen presentation (cf. ref. 40). Although class I molecules typically load peptides in the ER, several recent studies indicate that there are alternative pathways for peptide loading of class I outside the ER in which class I molecules bind peptide in either an endocytic vesicle in the cytosol (41) or at the plasma membrane (42). Furthermore, exogenous $\beta_2$m can promote peptide loading in both of these alternative pathways (14, 43). Binding of peptide and $\beta_2$m to class I molecules by these alternative pathways presumably must occur by exchange. The structural properties of $L^d$ render it highly susceptible to accepting exogenous peptide, and thus would facilitate its participation in these alternative pathways of antigen presentation. This feature could explain the prevalence of $L^d$ as a restriction element for a variety of immune T cells.

This work was supported by National Institutes of Health Grants 5R37 AI-07289, 1RO1 GM45839, 2PO1 AI-10792, 2P30 CA-13330, 1RO1 AI-27199, and AI19687 and assistance from the Wolfe–Welch Foundation.

1. Germain, R. N. & Margulies, D. H. (1993) *Annu. Rev. Immunol.* **11,** 403–450.
2. Bjorkman, P. J., Saper, M. A., Samraoui, B., Bennett, W. S., Strominger, J. L. & Wiley, D. C. (1987) *Nature (London)* **329,** 506–512.
3. Zhang, W., Young, A. C. M., Imarai, M., Nathenson, S. G. & Sacchettini, J. C. (1992) *Proc. Natl. Acad. Sci. USA* **89,** 8403–8407.
4. Fremont, D. H., Matsumura, M., Stura, E. A., Peterson, P. A. & Wilson, I. A. (1992) *Science* **257,** 919–927.
5. Young, A. C. M., Zhang, W., Sacchettini, J. C. & Nathenson, S. G. (1994) *Cell* **76,** 39–50.
6. Fremont, D. H., Stura, E. A., Matsumura, M., Peterson, P. A. & Wilson, I. A. (1995) *Proc. Natl. Acad. Sci. USA* **92,** 2479–2483.
7. Smith, K. J., Reid, S. W., Stuart, D. I., McMichael, A. J., Jones, E. Y. & Bell, J. I. (1996) *Immunity* **4,** 203–213.
8. Smith, K. J., Reid, S. W., Harlos, K., McMichael, A. J., Stuart, D. I., Bell, J. I. & Jones, E. Y. (1996) *Immunity* **4,** 215–228.
9. Bjorkman, P. J., Saper, M. A., Samraoui, B., Bennett, W. S., Strominger, J. L. & Wiley, D. C. (1987) *Nature (London)* **329,** 512–518.
10. Falk, K., Rötzchke, O., Stevanovic, S., Jung, G. & Rammensee, H.-G. (1991) *Nature (London)* **351,** 290–296.
11. Saper, M. A., Bjorkman, P. J. & Wiley, D. C. (1991) *J. Mol. Biol.* **219,** 277–319.
12. Ciavarra, R. & Forman, J. (1982) *J. Exp. Med.* **156,** 778–790.
13. Örn, A., Goodenow, R. S., Hood, L., Brayton, P. R., Woodward, J. G., Harmon, R. C. & Frelinger, J. A. (1982) *Nature (London)* **297,** 415–417.
14. Schirmbeck, R., Melber, K. & Reinman, J. (1995) *Eur. J. Immunol.* **25,** 1063–1070.
15. Reddehase, M. J., Buhring, H.-J. & Koszinowski, U. H. (1986) *J. Virol.* **57,** 408–412.
16. Hansen, T. H. & Levy, R. B. (1978) *J. Immunol.* **120,** 1836–1840.
17. Beck, J. C., Hansen, T. H., Cullen, S. E. & Lee, D. R. (1978) *J. Immunol.* **137,** 916–923.
18. Townsend, A., Elliot, T., Cerundolo, V., Foster, L., Barber, B. & Tse, A. (1990) *Cell* **62,** 285–295.
19. Corr, M., Boyd, L. F., Frankel, S. R., Kozlowski, S., Padlan, E. A. & Margulies, D. H. (1992) *J. Exp. Med.* **176,** 1681–1692.
20. Barber, L. D., Gillece-Castro, B., Percival, L., Li, X., Clayberger, C. & Parham, P. (1995) *Curr. Biol.* **5,** 179–190.
21. Udaka, K., Tsomides, T. J. & Eisen, H. N. (1992) *Cell* **69,** 989–998.
22. McCormick, D., Stauss, H. J., Thorpe, C., Travers, P. & Dyson, P. J. (1996) *Eur. J. Immunol.* **26,** 2895–2902.
23. Jancarik, J. & Kim, S.-H. (1991) *J. Appl. Crystallogr.* **24,** 409–411.
24. Navaza, J. (1994) *Acta Crystallogr. A* **50,** 157–163.
25. Brunger, A. T. & Krukowski, A. (1990) *Acta Crystallogr. A* **46,** 585–593.
26. Tronrud, D. E., Ten Eyck, L. F. & Matthews, B. W. (1988) *Acta Crystallogr A.* **43,** 489–501.
27. Smith, J. D., Myers, N. B., Gorka, J. & Hansen, T. H. (1993) *J. Exp. Med.* **178,** 2035–2046.
28. Myers, N. B., Lie, W.-R., Nett, M., Rubocki, R. J. & Hansen, T. H. (1989) *J. Immunol.* **142,** 2751–2758.
29. Robinson, R. A. & Lee, D. R. (1996) *J. Immunol.* **156,** 4266–4273.
30. Sun, R., Shepard, S. E., Geier, S. S., Thomson, C. T., Sheil, J. M. & Nathenson, S. G. (1995) *Immunity* **3,** 573–582.
31. Garcia, K. C., Degano, M., Stanfield, R. L., Brunmark, A., Jackson, M. R., Peterson, P. A., Teyton, L. & Wilson, I. A. (1996) *Science* **274,** 209–219.
32. Nicholls, A., Sharp, K. & Honig, B. H. (1991) *Proteins* **11,** 281–296.
33. Young, A. C. M., Nathenson, S. G. & Sacchettini, J. C. (1995) *FASEB J.* **9,** 26–36.
34. Connolly, J. M. (1994) *Proc. Natl. Acad. Sci. USA* **91,** 11482–11486.
35. Lurguin, C., Van Pel, A., Maraime, B., Deplaen, E., Szikora, J.-P., Janssens, C., Reddehase, M. J., Lejeune, J. & Boon, T. (1989) *Cell* **58,** 293–303.
36. Townsend, A., Ohlen, C., Bastin, J., Ljunggren, H.-G., Foster, L. & Karre, K. (1989) *Nature (London)* **340,** 443–448.
37. Lie, W.-R., Myers, N. B., Gorka, J., Rubocki, R. J., Connolly, J. M. & Hansen, T. H. (1990) *Nature (London)* **344,** 439–441.
38. Ortman, B., Androlewicz, M. & Cresswell, P. (1994) *Nature (London)* **368,** 864–867.
39. Suh, W.-K., Cohen-Doyle, M. F., Fruh, K., Wang, K., Peterson, P. A. & Williams, D. B. (1994) *Science* **264,** 1322–1326.
40. Jondal, M., Schirmbeck, R. & Reinmann, J. (1996) *Immunity* **5,** 295–302.
41. Kovacsovics-Bankowski, M. & Rock, K. L. (1995) *Science* **269,** 1585–1587.
42. Pfeifer, J. D., Wick, M. J., Roberts, R. L., Fidlay, K., Normark, S. J. & Harding, C. V. (1993) *Nature (London)* **361,** 359–361.
43. Vitiello, A., Potter, T. A. & Sherman, L. A. (1990) *Science* **250,** 1423–1426.